

Composite Graphene-Modified Aluminum Foil Cathode Current Collectors for Lithium-ion Battery with Enhanced Mechanical and Electrochemical Performances

Yao Zhou,^[a, b, c] Huiqi Wang,^{*[b]} and Junying Wang^{*[a, c]}

Aluminum foil is a typical cathode collector in lithium-ion batteries, yet it encounters various issues, including restricted contact with the active substance, poor adhesion, and regional corrosion associated with the electrolyte. Although conventional carbon-coated aluminum foils partially alleviate such problems, they suffer from excess weight and thickness of their carbon layers. Here a simple casting method to prepare Ketjen Black/aqueous graphene dispersion slurry modified aluminum foil (KB-AGD-Al-CCs) and graphene micro-sheets/aqueous graphene dispersion slurry modified aluminum foil (GM-AGD-Al-CCs). Our results indicate that batteries utilizing graphene-modified aluminum foils exhibited superior electrochemical performance compared with that of carbon-coated aluminum

foils. The lithium-ion battery employing GM-AGD-Al-CCs as cathode current collectors exhibits reversible specific capacities of 155, 118, and 92.5 mAh/g at current densities of 0.1, 5, and 10 C. After cycling for 1800 cycles at 5 and 10 C, its specific capacities remain at 91 and 77.5 mAh/g. Combing contact angle measurement, electrical conductivity test with electrochemical impedance spectroscopy indicates that the graphene coating decreases the contact angle between the commercial LiFePO₄ and current collector, increases the electrical conductivity of the electrode and adhesion. Moreover, the inclusion of GM and KB as conductive additives compensates for graphene's low interlayer conductivity by forming a conductive network.

Introduction

With the development of modern consumer electronics and new energy vehicle industry, lithium-ion batteries (LIBs) have been put forward higher performance requirements, such as higher capacity and rate capability, more safety and longer life.^[1] The current collector is a crucial component of LIBs, responsible for loading electrode materials and transmitting current to enable proper performance.^[2] Aluminum foil has become the most commonly employed cathode electrode current collector material due to its cost-effectiveness, stability of electrochemical and chemical properties, and high electrical conductance.^[3] However aluminum foil as a current collector encounters numerous challenges. The smooth surface of aluminum foil restricts the contact area and adhesion between the electrode material and the current collector. This not only results in a greater interfacial contact resistance, but also increases the likelihood of detachment of electrode materials

throughout battery cycling, thus accelerating battery capacity degradation.^[4] At the same time, corrosion between the aluminum foil and electrolyte during extended cycling also presents a significant issue.^[5] This illustrates that ordinary aluminum foils struggle to meet the high-performance LIB requirements.

In order to increase the contact area and adhesion between the electrode material and the current collector, the surface of the aluminum foil is chemically or electrochemically etched to increase the surface roughness, which provides a larger contact area between the electrode material and the current collector, and to a certain extent improves the adhesion between the two, reduces the internal resistance, improves the rate capability, and prolongs the cycling life, however, this operation inevitably reduces the mechanical properties of the foil.^[6] Meanwhile, numerous studies have reported on the regulation of electrolyte composition to prevent surface corrosion of aluminum foils. LiPF₆-based electrolytes have the ability to create a safeguarding layer of aluminum fluoride on the surface of alumina during the initial phase of battery cycle, which in turn prevents further corrosion of aluminum foils.^[7] Nonetheless, it should be noted that neither the naturally occurring alumina layer nor the artificially induced aluminum fluoride layer can sustain resistance to corrosion for extended periods, particularly under a high voltage of 3.0 V. The constituents within the electrolyte initiate a reaction with the alumina resulting in the production of unconfined Al₃⁺. These ions have the capability to dissolve and migrate into the electrolyte, consequently aggravating the phenomenon of corrosion.^[8] The utilization of super-concentrated imide as an electrolyte suppresses the formulation and dissolution of aluminum

[a] Y. Zhou,⁺ J. Wang
CAS Key Laboratory of Carbon Materials, Institute of Coal Chemistry,
Chinese Academy of Sciences, Taiyuan 030001

[b] Y. Zhou,⁺ H. Wang
College of Energy and Power Engineering, North University of China,
Taiyuan 030051
E-mail: hqiwang@nuc.edu.cn

[c] Y. Zhou,⁺ J. Wang
Center of Materials and Opto-Electronic, University of Chinese Academy of
Sciences, Beijing 100049, China
E-mail: wangjy@sxicc.ac.cn

 Supporting information for this article is available on the WWW under
<https://doi.org/10.1002/batt.202400028>

complexes by decreasing solvent molecules or free anions in the electrolyte system. This results in effective control over the corroding phenomenon. Nonetheless, this method comes at a high cost and imposes stringent technical requirements. It also compromises the conductivity of the electrolyte, thus influencing the overall battery performance.^[9]

In recent times, the cathode electrode current collector of commercial batteries has found extensive use of carbon coated aluminum foil.^[10] The improved conductive carbon coating increases the contact area between the electrode material and the current collector, enhances adhesion, reduces electrical resistance, and inhibits polarization during the charging and discharging cycle. Additionally, it protects the surface of the aluminum foil, preventing corrosion and improving the cycle life of the battery.^[11] Nevertheless, the substances employed to cover the carbon layer tend to be carbon black or graphite, both of which are usually thicker (2–5 µm) and occupy a significant amount of electrode mass and area, consequently impacting the battery's specific capacity and energy density.

Graphene possesses a large specific surface area, high electrical conductivity, and is lightweight, making it an ideal material for a new carbon coating. The use of plasma-enhanced chemical vapor precipitation (PECVD) graphene for armoring aluminum foils results in modified foils that exhibit exceptional electrochemical properties, including more stable cycle life, better rate performance, and specific capacity.^[12] Nevertheless, the method requires complex technical conditions, making large-scale development and application challenging. In contrast, the reduction of graphene oxide (RGO) at a technical level requires less complexity, but the process of preparing and dispersing graphene still poses significant difficulties.^[13]

In this study, we investigate AGD-Al-CCs, an aqueous graphene dispersion slurry-enhanced anode current collector, for LiFePO₄ (LFP) lithium-ion batteries. The process involves forming a coating of graphene on commercial aluminum foils by applying a graphene aqueous dispersion. Additionally, the electrical conductivity of the graphene coating is enhanced by adding graphene microsheets (GM-AGD-Al-CCs) or Ketjen Black (KB-AGD-Al-CCs). The aluminum foils modified with graphene, exhibit improved electrochemical properties. These include reduced internal resistance and mass, increased capacity and rate performance, and improved cycling stability and mechanical strength. These advancements may lead to novel opportunities for enhancing the functioning of lithium-ion batteries.

Experimental Section

Preparation of AGD-Al-CCs, GM-AGD-Al-CCs and KB-AGD-Al-CCs

A specified quantity of sodium carboxymethyl cellulose (CMC) was dissolved in deionized water in multiple batches and subjected to magnetic stirring at 60 °C for 2 h. This resulted in the formation of a clear, viscous liquid with a concentration of 1.3 wt%. Subsequently, the aqueous graphene (GPE) dispersion with a concentration of 5 wt% was mixed with the CMC liquid in a 2:1 ratio based on solid content, followed by 1 h ball milling. Afterward, Styrene butadiene

rubber (SBR, 49.8%) was then added to a mixture of graphene and CMC, where GPE:CMC:SBR = 2:1:1.46, the mixture was ball milled for 1 hour to produce aqueous graphene dispersion slurry (AGD).

The preparation of GM-AGD and KB-AGD followed a process similar to AGD, with the additional step of introducing GM and KB separately before adding butadiene rubber. In this case, GM accounted for a total solid content of 1.5%, 2%, and 2.5%, while KB accounted for a total solid content of 2.5% in the dispersion.

The three slurries were blade coated on 16 µm aluminum foil using an SZQ four-roll coater and then dried in a vacuum oven at 60 °C for 2 h. LFP:PVDF:KB = 8:1:1, along with a specified amount of N-Methyl-pyrrolidone (NMP, 99%), was uniformly coated onto the modified aluminum foil. The coated aluminum foils were then dried in a vacuum oven at 60 °C for 24 h. The electrodes (circular shape with diameter of 12 mm) were fabricated into half cells with lithium metal electrodes, membrane (2325, Celgard), electrolyte (E706.100.038, 1.0 M LiPF₆ in EC:DMC:EMC = 1:1:1, Suzhou Duo-doo Chemical Technology Co., Ltd), and button cell modules (CR 2016, shanghai Yiming)

Physicochemical Property Measurements

Tensile strength tests were conducted using the UTM2103 electronic universal testing machine from Shenzhen Sansi Zhong-heng Technology Co., Ltd. The modified aluminum foils were cut into standard dimensions of 150 mm×15 mm, leaving 10 mm at the top and bottom as clamping positions.

Contact angle measurements were performed using the JC2000DM contact angle measurement instrument from Shanghai Zhong Chen Technology Equipment Co., Ltd. Suitable samples of AGD-Al-CCs, GM-AGD-Al-CCs, KB-AGD-Al-CCs, and Al-CCs were selected for testing. The test reagent used was a secondary lithium-ion battery electrolyte (1.0 M LiPF₆ in EC:DMC:EMC = 1:1:1). Electrical conductivity testing was carried out using the RTS-9 four-point probe tester (double-electrode four-point probe) from Guangzhou Sitanz-heng Technology Co., Ltd.

Characterization and Electrochemical Properties Measurements

Morphological analysis was conducted using the scanning electron microscope (SEM JSM-7001F) from JEOL, Japan. X-ray diffraction (XRD) analysis was performed using the D8 ADVANCE A25 X-ray powder diffractometer from Germany. The Bragg measurement method was employed to characterize the structure of powder samples within the range of 10° to 90°. The geometric shape of the measurement area was circular with a diameter of 10 mm.

Electrochemical performance was tested using cyclic voltammetry (CV), galvanostatic charge-discharge (GCD), and electrochemical impedance spectroscopy (EIS). GCD and EIS tests were conducted at ambient temperature using the battery test system (CT2001A) from Wuhan Land Electronics Co., Ltd. GCD tests were performed at different current densities (1–10 C) with LFP nominal capacity (170 mAh/g). EIS measurements were conducted within a frequency range of 100 KHz to 0.01 Hz. Cyclic voltammetry (CV) was performed using the AUT50021 electrochemical analyzer from Metrohm, Switzerland, with a scan rate of 1 mV (2.4–4.2 V) to obtain CV spectra.

Results and Discussion

The Morphology of Graphene

Figure 1a illustrates the morphology of graphene, which was produced through electrochemical exfoliation, it has clear edges, is 1–4 layers thick and has good dispersion.^[12] More detailed, the number of prepared graphene layers is less than 6 layers, with 32% of them being comprised of two layers and 25% being comprised of three layers (Figure S1). Figure S2 shows the Raman analysis of the prepared graphene, whose 2D peaks can be fitted as three Lorentzian peaks representing 4 layers of graphene.^[14] XRD shows two diffraction peaks at 26.61° and 46.3°, corresponding to the (002) and (004) crystal planes of carbon (Figure S3).

Figure 1b shows the morphology of the bare aluminium foil, which has a smooth and flat surface without contamination. The prepared graphene slurry was blade coated on aluminum foil by SZQ four-roll coater. After drying, a graphene layer with a uniform distribution and a minimum thickness of 1.6 μm is formed (Figure 1c&Figure S4). GM was added as a conductive additive to the graphene slurry. It was well dispersed in the graphene slurry, as shown in Figure 1d. Figure 1e shows the topography of GM with sizes less than 500 nm. LiFePO₄ as

cathode active substance coated on modified aluminum foils as shown in Figure 1f.

Contact Angle Test with Different Fluid Collectors

The wetting ability of the current collector with the electrolyte is a crucial factor that impacts battery performance.^[15] As demonstrated in Figure 2, contact angle tests were conducted on carbon-coated aluminum foil, GM-AGD-Al-CCs, and KB-AGD-Al-CCs to investigate their wettability with the electrolyte. Figure 2 shows that the contact angle of GM-AGD-Al-CCs is 14.2°, which is lower than the corresponding angles of 18.4° observed for KB-AGD-Al-CCs and 22.6° for carbon coated aluminium foils. This suggests that the graphene-modified aluminium foils have smaller contact angles compared to carbon coated aluminium foils due to the larger specific surface area of the graphene layer which increases the contact area between the electrolyte and the current collector, thus improving the wettability of the current collector.^[16] We also measured the contact angle of the LFP cathode paste with the current collector, and the modified current collector also demonstrated good wettability (Figure S5). These findings demonstrate the beneficial effect of graphene in enhancing the

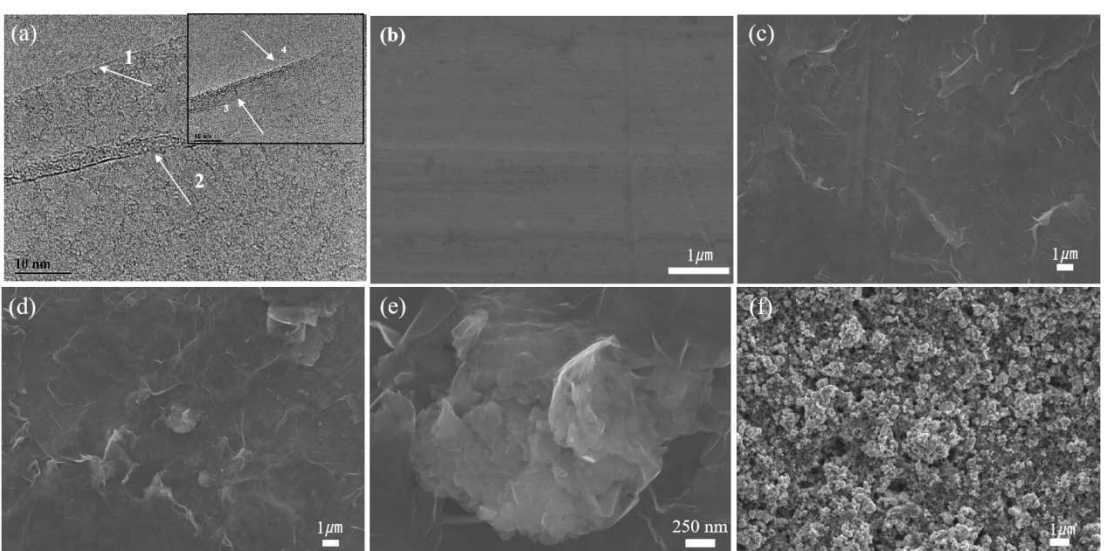


Figure 1. Al-CCs morphology. (a) Morphology of graphene with different layers and (b) bare Al CCs, (c) AGD-Al-CCs, (d) GM-AGD-Al-CCs. (e) Morphology of GM. (f) LiFePO₄ on modified Al CCs.



Figure 2. Contact angle of Al-CCs. (a) Carbon coated Al-CCs. (b) KB-AGD-Al-CCs and (c) GM-AGD-Al-CCs.

wettability of the current collector-electrolyte and LFP cathode slurry.

Electrical Conductivity Testing of Different Collectors

The electrical conductivity of graphene-modified current collector is regulated by the composite coating on its surface, and the electrical conductivity of the current collector plays a crucial factor in the performance of the battery.^[17] Therefore, we conducted investigations into the respective electrical conductivities of GM-AGD-Al-CCs, KB-AGD-Al-CCs, and carbon-coated aluminum foils. Figure 3a shows the electrical conductivities of three modified current collectors, where 7 samples of each current collector type were tested and averaged. The results showed that GM-AGD-Al-CCs had the highest conductivity with an average of 50 S/cm, which was greater than KB-AGD-Al-CCs with an average of 20 S/cm, whereas carbon-coated aluminium foils had the lowest conductivity of 12 S/cm. This is due to the high electrical conductivity of graphene.^[18] It was observed that the addition of GM and KB to the graphene slurry resulted in a significant difference in electrical conductivity. The unique spherical branched chain structure of Ketjen Black (KB) can improve the shortcomings of poor vertical electrical conductivity of graphene to a certain extent. When GM is completely mixed with graphene slurry, it can form a conducting network

with graphene more effectively due to its unique small-size lamellar structure. Therefore, its electrical conductivity is superior.^[19]

So far, we've confirmed that GM-AGD-Al-CCs have demonstrated greater electrical conductivity than both the carbon coated aluminum foil and the KB-AGD-Al-CCs. In order to verify the relationship between the thickness of the graphene coating and the electrical conductivity of the modified current collector further, a series of electrical conductivity tests were performed using a GM-AGD-Al-CCs with varying wet film thicknesses, as depicted in Figure 3b. The highest electrical conductivity value of 52 S/cm is observed at a thickness of 50 µm. However, as the thickness increases to 100 µm, the electrical conductivity decreases to 32 S/cm, at thicknesses of 150 µm and 200 µm, the electrical conductivities reduce to 17 S/cm and 5 S/cm respectively. These results indicate that thin-layered graphene offers a considerable advantage in terms of electrical conductivity. However, it is worth noting that the electrical conductivity of graphene-modified aluminium foils without any conductive additives is still very low, despite a wet film thickness of only 50 µm, its electrical conductivity is just 0.3 S/cm, which is less than one-tenth of the same thickness but with the inclusion of conductive additives. This study confirms the possibility of enhancing the vertical electrical conductivity of graphene through the incorporation of conductive additives of varying

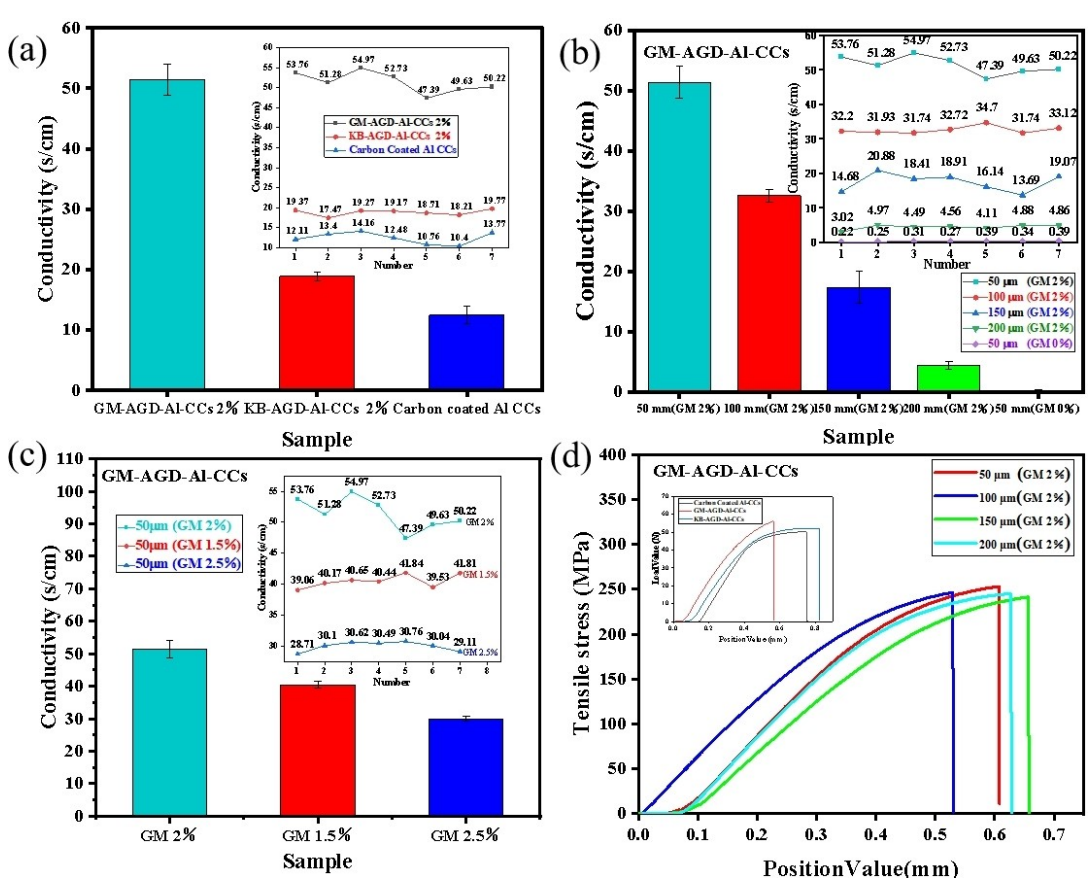


Figure 3. Electrical conductivity and mechanical strength of modified Al-CCs. Electrical conductivity of (a) GM-AGD-Al-CCs, KB-AGD-Al-CCs, and Carbon Coated Al-CCs. (b) GM with different wet film thicknesses. (c) Al CCs with different GM additions. (d) Tensile strength of GM with different wet film thicknesses.

sizes, thus building a network that conducts electricity efficiently.^[20]

The electrical conductivity test confirmed the effectiveness of GM as a conductive additive in enhancing the electrical conductivity of graphene coating. However, the electrical conductivity is also related to the amount of conductive additive added. To evaluate this, we examined the impact of different amounts of GM added to graphene slurry, with GM solid content of 1.5%, 2%, and 2.5%, respectively. Figure 3c illustrates the electrical conductivities of the three samples tested. It is evident that the highest electrical conductivity, at 52 S/cm, was achieved with 2% GM, followed by 40 S/cm with 1.5% GM, the lowest electrical conductivity was recorded with 2.5% GM. We find that there is no positive correlation between electrical conductivity and the quantity of GM added. Electrical conductivity increases when a small amount of GM is added but decreases when the amount of GM added exceeds a certain amount. This may be due to that a conductive additive content of 1.5% is too small to form an adequate conductive network. With an increase in the amount of additive, the electrical conductivity of the conductive network improves, until a point of optimal composition is reached at 2%. The decrease in electrical conductivity may be due to an increase in the addition of conductive additive, which are not sufficiently dispersed. The composition of the conductive network may be too complex, which affects the electron transport path.^[21]

Mechanical Strength Testing of Different Collectors

The mechanical strength of the current collector is an important indicator.^[22] Figure 3d shows the tensile strength of AGD-Al-CCs, carbon coated aluminum foil and KB-AGD-Al-CCs at various wet film thicknesses (The load value at break indicates the mechanical strength). We can see that GM-AGD-Al-CCs possesses the largest breaking load of 56 N, which is higher than that of KB-AGD-Al-CCs of 52 N and that of carbon-coated aluminium foils of 50 N. Graphene's hybridized sp₂ orbitals

connect its carbon-carbon bonds, while its solid six-membered benzene ring contributes to its structure and stability.^[23] As a result, graphene boasts the highest mechanical strength of any new nanomaterial in history, making the graphene composite slurry coating on aluminum foils an effective strategy for improving its mechanical properties.

In addition to the type of coating, the thickness of the coating is also an important factor affecting the mechanical strength.^[24] We conducted a comparison of the tensile strengths of GM-AGD-Al-CCs with varying wet film thicknesses, using tensile stress as the test index. The optimal mechanical strength was found at a wet film thickness of 50 μm, displaying a tensile stress of 253 MPa, exceeding that of 246 MPa at a wet film thickness of 100 μm, 241 MPa at a wet film thickness of 150 μm, and 244 MPa at a wet film thickness of 200 μm. These tests reflect the excellent mechanical properties of thin-layered graphene.

Electrochemical Performance of Half-Cells

Half cells are assembled to investigate the electrochemical performances of the LFP LIBs with GM-AGD-Al-CCs, KB-AGD-Al-CCs and carbon-coated aluminum foils as current collectors. The rate capability and cycle profiles in Figure 4a–e reveal that LIBs of GM-AGD-Al-CCs possess the best electrochemical performances compared with those of KB-AGD-Al-CCs and carbon-coated aluminum foils. During long term cycling demonstrated in Figure 4a–b, the LIBs of GM-AGD-Al-CCs maintain higher specific capacities at both 5 C and 10 C. After 1800 cycles at the rate of 5 C, the specific capacity of GM-AGD-Al-CCs maintain 91 mAh/g with the capacity retention ratio of 81.2% higher than that of KB-AGD-Al-CCs (82.4 mAh/g, 77.1%), and carbon-coated aluminum (33 mAh/g, 41.6%), suggesting the good cycling performance. GM-AGD-Al-CCs also exhibit much higher capacity retention ratio and cycling stability at higher rate (e.g. at a rate of 10 C), revealing superior rate performance. Also, GM-AGD-Al-CCs exhibited the highest

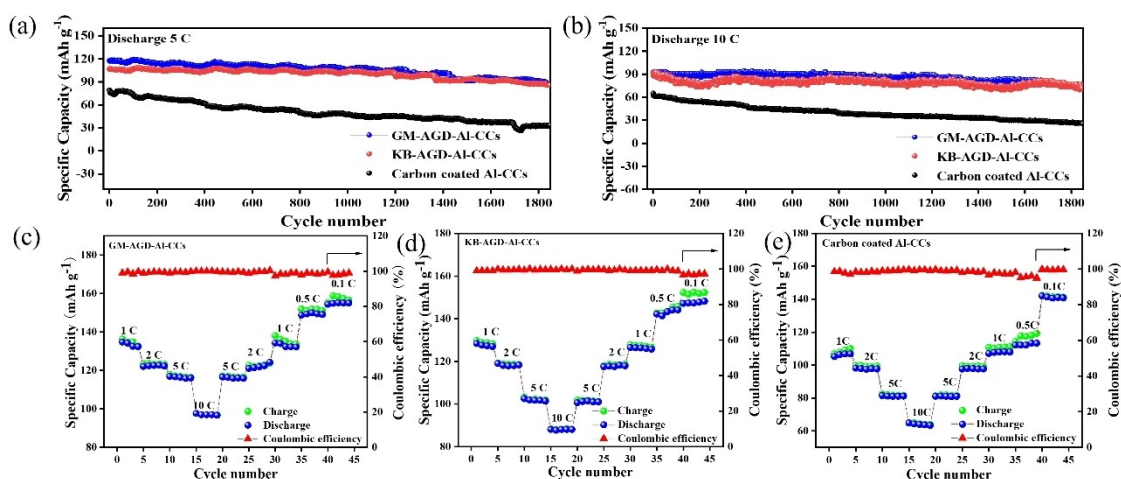


Figure 4. Electrochemical performance of modified Al-CCs. (a–b) Long cycling tests of different modified Al-CCs. (c–e) Rate performance tests of different modified Al-CCs.

specific capacity at a current density of 1 C (Figure S6). The study showed that the current collector modified with graphene exhibits enhanced capacity and cycling stability as compared to the carbon-coated aluminum foil at high current density.^[25] This is attributed to the large specific surface area of graphene and the increased contact area and adhesion between the active substance and the aluminum foil through the graphene coating.^[26] Figure S7 shows the nitrogen adsorption and desorption curves of graphene and conductive carbon black (the coating on the surface of the carbon-coated aluminium foil). According to the calculation, it can be seen that graphene has a specific surface area of $398 \text{ m}^2/\text{g}$, while the conductive carbon black has a specific surface area of only $23.95 \text{ m}^2/\text{g}$, which indicates that the introduction of the graphene coating can significantly increase the specific surface area of the current collector compared to that of the carbon coated aluminium foil. Compared to typical carbon coatings, it has better electrical contact and charge transfer phenomena. In order to better verify the protective effect of graphene coating on the current collector at high voltage, we are using Li-NiCoO₂ (NMC622) as the cathode material to test the GM-AGD-Al-CCs at a voltage range of 2.8–4.3 V vs. Li/Li⁺, which also showed good performance as shown in Figure S8.

To diagnose the anodic corrosion properties of graphene-modified current collector, we carried out electrochemical tests of the carbon coated aluminium foil and GM-AGD-Al-CCs. Briefly, 2016-type coin cells were fabricated by using GM-AGD-Al-CCs (or carbon coated aluminium foil) as positive electrode and lithium foil as counter/reference electrode (i.e., GM-AGD-Al-CCs (or carbon coated aluminium foil)/electrolyte/Li) for cyclic voltammetry (CV) examination (3.5–4.5 V vs. Li/Li⁺). 50 μL electrolyte (1 M LiPF₆) was standardly added for each cell. Figure S8 shows the morphology of the current collector after CV cycling, and it can be seen that the GM-AGD-Al-CCs survived stably without any obvious changes (Figure S9a), while the carbon layer on the surface of the carbon-coated aluminium foil has already peeled off (Figure S9b).

Furthermore, the EIS results depicted in Figure 5b validate this conclusion. The Nyquist plot displays a semicircle at high frequencies and a straight line at low frequencies, indicating the charge transfer resistance (R_{ct}) at the interface of the

electrode and electrolyte, and the Warburg impedance (W_0) caused by the diffusion of Li⁺ in the electrodes, respectively.^[27] Though the mediation of graphene has no distinct influence on diffusion in electrodes, the application of graphene coating resulted in a reduced R_{ct} of the GM-AGD-Al-CCs as compared to the carbon-coated aluminum foil because of the improved electrical contact between electrode materials and current collectors. The R_{ct} value for GM-AGD-Al-CCs is 112.5Ω , which is lower than the R_{ct} value for KB-AGD-Al-CCs (187.6Ω) and carbon coated aluminium foils (200.6Ω). Obviously, the internal resistance of half-cells assembled by a current collector modified with graphene is lower than that of the unmodified current collector. The modification reduces the interface resistance between the aluminum foil and LFP and optimizes the electron transport path, increasing electron collection ability and improving electrochemical power. The R_{ct} value of the graphene-modified aluminum foil without GM or KB is 494Ω (Figure S10), significantly higher than that of the three aforementioned current collectors. Although graphene coatings can improve electrical contact by enlarging the contact surface between LFP electrodes and current collectors, the insufficient interlayer electrical conductivity of graphene may impede vertical interlayer charge transfer.^[28] The incorporation of GM enhances the electrical conductivity of graphene in the vertical direction compared to KB. This result is consistent with the electrical conductivity tests conducted on the three current collectors depicted in Figure 4a. As can be seen in the CV cycling diagram presented in Figure 5a, GM-AGD-Al-CCs and KB-AGD-Al-CCs have a larger redox peak area than the carbon-coated aluminium foils, indicating a larger electrochemically active area. Meanwhile, the redox peak distances of GM-AGD-Al-CCs and KB-AGD-Al-CCs are smaller than those of carbon coated-Al-CCs, indicating their lower polarization phenomena.

To assess the rate performance of the three current collectors, we conducted successive charging and discharging at the rates of 0.1 C, 0.5 C, 1 C, 2 C, 5 C, and 10 C. The rate performance of the three current collectors is displayed in Figure 4c-d. We observe that the graphene-modified current collector exhibits significantly lower capacity decay than the carbon-coated aluminum foil under various consecutive current densities. Figure 6a-c show the charge-discharge curves of the

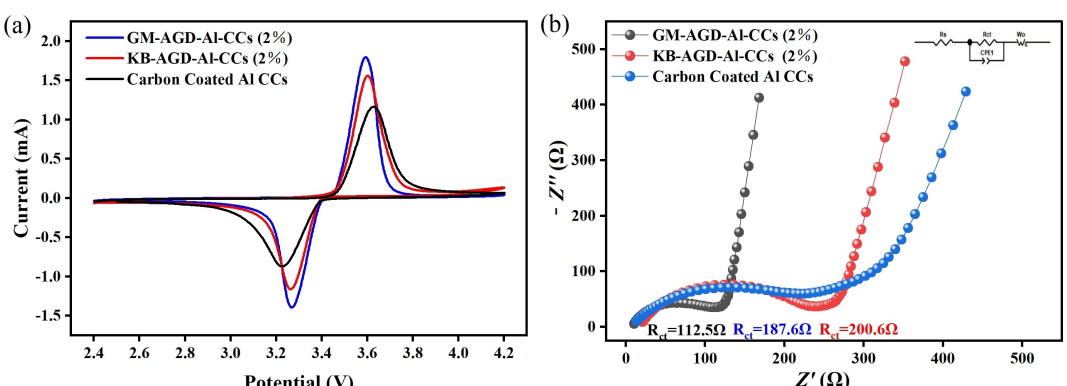


Figure 5. The electrochemical performance of the half-cell assembled using three types of fluid current collectors: (a) CV cycle diagram, and (b) electrochemical impedance diagram.

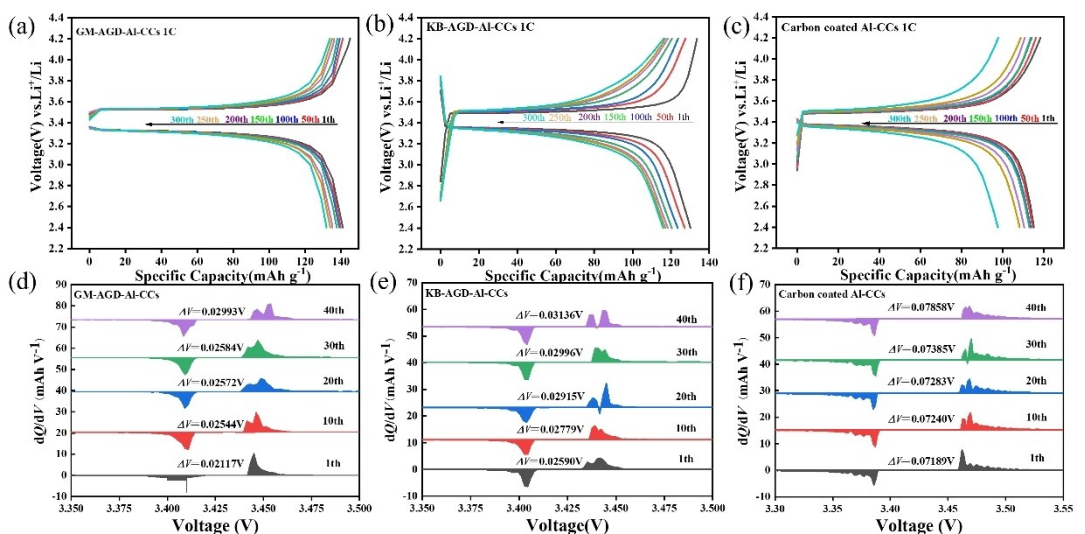


Figure 6. Electrochemical performance of modified Al-CCCs. (a–c) Charge-discharge curves at different cycle times. (d–f) The dQ/dV plots of the cells that were prepared under various charge-discharge cycles at 1 C.

three types of current collectors at a current density of 1 C for different numbers of cycles, it can be seen that after 300 charge-discharge cycles, these three types of current collectors have different degrees of capacity decay, with the capacity retention of GM-AGD-Al-CCCs being 93.5%, which is higher than that of KB-AGD-Al-CCCs, which is 89.1%, and much higher than that of carbon coated aluminium foil, which is 84.8%.

The dQ/dV curve depicts the voltage fluctuation of the electrode material in the unit capacity range and can provide an elaborate description of cell capacity decay and polarization phenomena.^[29] The charge-discharge curves show two plateaus at 3.4 V and 3.5 V, respectively, corresponding to the discharge and charge plateaus of the LFP cathode. The polarisation phenomenon of a cell is usually manifested as a separation of these two voltage plateaus.^[30] Figure 6d–f exhibits the dQ/dV curve of the battery consisting of three current collectors types operating at 0.1 C current density. It can be seen that as the number of cycles increases, after 40 cycles, the platform gap between the charging and discharging points of the battery using GM-AGD-Al-CCCs is 29.93 mV, which is lower than that of KB-AGD-Al-CCCs (31.36 mV) and carbon coated aluminium foil (78.58 mV). This shows a lower potential polarization of the cells using GM-AGD-Al-CCCs, which is also consistent with the conclusions drawn in Figure 6a–c. It is noteworthy that the performance of the graphene-modified current collector is significantly better than that of the carbon-coated aluminium foil in high current density conditions compared to low current density ones. This is due to the enlarged contact area between the electrode material and the active material caused by the graphene coating, which enhances the bonding force between them. As a result, this reduces the occurrence of active material detachment and current collector corrosion by the electrolyte during high current density charging and discharging, thus averting rapid capacity decay.^[31] The charge-discharge curves depicted in Figure S11 also confirm this point.

Conclusions

In conclusion, this study presents a composite graphene coating that is highly conductive and controllable. It has been applied to cathode current collectors of lithium-ion batteries and has demonstrated high electrochemical stability when compared to conventional carbon-coated aluminium foils. Using assembly-based half-cell tests, it was found that cathode current collectors made of GM-AGD-Al-CCCs and KB-AGD-Al-CCCs have both significantly improved electrochemical performance in terms of capacity, rate performance, and cycling stability.

The observations can be attributed to the impact of graphene coating as follows: Firstly, the coating heightens the adhesion between the electrode materials and the current collector on the aluminium foil, thereby augmenting their electrical contact and charge transfer. Secondly, the graphene coating effectively thwarts the electrolyte corrosion of the current collector during prolonged cycling. On the flip side, overly abundant graphene flake layers on the aluminium foil's surface can reduce LIB performance because the excessive coating thickness hinders the vertical electrical conductivity of graphene. Incorporating GM and KB alongside the graphene flakes forms a conducting network that counterbalances the low inter-layer electrical conductivity of graphene and enables charge transfer, resulting in enhanced electrochemical performance. This work develops a facile method to prepare graphene-modified Al foils, which acts as the novel current collectors with lighter and thinner coatings for higher performances LIBs.

Author Contributions

Yiao Zhou: Conceptualization, Methodology, Validation, Data curation, Writing – original draft. **Huiqi Wang:** Supervision, Resources, review & editing. **Junying Wang:** Project administration, Funding acquisition, Supervision, review & editing.

Acknowledgements

This work was supported by the National Natural Science Foundation of China (22179138), the Natural Science Foundation of Shanxi Province (2021030212300).

Conflict of Interests

The authors declare that they have no known competing financial interests or personal relationships that could have appeared to influence the work reported in this paper.

Data Availability Statement

Data will be made available on request.

Keywords: Cathode current collector • Electrochemistry • Graphene • Enhanced performances • Lithium-ion battery

- [1] a) J. B. Goodenough, K.-S. Park, *J. Am. Chem. Soc.* **2013**, *135*, 1167–1176; b) G. Kucinskas, G. Bajars, J. Kleperis, *J. Power Sources* **2013**, *240*, 66–79;
- c) Z. Zhu, T. Mankowski, K. Balakrishnan, A. S. Shikoh, F. Touati, M. A. Benammar, M. Mansuripur, C. M. Falco, *ACS Appl. Mater. Interfaces* **2015**, *7*, 16223–16230.
- [2] X. Yang, X. Li, K. Adair, H. Zhang, X. Sun, *Electrochem. Energy Rev.* **2018**, *1*, 239–293.
- [3] S. S. Zhang, T. R. Jow, *J. Power Sources* **2002**, *109*, 458–464.
- [4] R. Kondo, T. Kikuchi, S. Natsui, R. O. Suzuki, *Mater. Lett.* **2016**, *183*, 285–289.
- [5] M. A. Deyab, G. Mele, E. Bloise, Q. Mohsen, *Sci. Rep.* **2021**, *11*, 12371.
- [6] K. R. Crompton, M. Hladky, *ACS Appl. Energ. Mater.* **2021**, *4*, 5511–5532.
- [7] X. Y. Zhang, T. M. Devine, *J. Electrochem. Soc.* **2006**, *153*, B344–B351.
- [8] E. Kramer, S. Passerini, M. Winter, *ECS Electrochem. Lett.* **2012**, *1*, C9–C11.
- [9] a) W.-h. Hou, Y. Lu, Y. Ou, P. Zhou, S. Yan, X. He, X. Geng, K. Liu, *Trans. Tianjin Univ.* **2023**, *29*, 120–135; b) F. Ahmed, I. Choi, T. Ryu, S. Yoon, M. M. Rahman, W. Zhang, H. Jang, W. Kim, *J. Power Sources* **2020**, *455*, 227980.
- [10] a) Z. Zhong, L. Kong, S. Huang, W. Shang, R. Zhang, L. Chen, *New Chem. Mater.* **2020**, *48*, 189–192; b) C. X. Ma, X. N. Wang, Y. J. Song, H. Y. Hu, W. Li, Z. J. Qiu, Y. P. Cui, W. Xing, *Asia-Pac. J. Chem. Eng.* **2023**, *18*, e2841.
- [11] T. Li, H. Bo, H. Cao, Y. Lai, Y. Liu, *Int. J. Electrochem. Sci.* **2017**, *12*, 3099–3108.
- [12] J. Wang, J. Huang, R. Yan, F. Wang, W. Cheng, Q. Guo, J. Wang, *J. Mater. Chem. A* **2015**, *3*, 3144–3150.
- [13] Y. Y. Li, J. Y. Wang, Z. H. Tian, F. L. Lai, T. X. Liu, G. J. He, *Batteries & Supercaps* **2023**, *6*, e202200509.
- [14] Z. H. Ni, Y. Y. Wang, T. Yu, Z. X. Shen, *Nano Res.* **2008**, *1*, 273–291.
- [15] a) M.-S. Wang, Z.-Q. Wang, Z.-L. Yang, Y. Huang, J. Zheng, X. Li, *Electrochim. Acta* **2017**, *240*, 7–15; b) L. Wen, J. Liang, C.-M. Liu, J. Chen, Q.-g. Huang, H.-z. Luo, F. Li, *J. Electrochem. Soc.* **2016**, *163*, A2951–A2955; c) L. Zhao, Y. Li, M. Yu, Y. Peng, F. Ran, *Adv. Sci.* **2023**, *10*, e2300283.
- [16] a) C. U. Jeong, S.-Y. Lee, J. Kim, K. Y. Cho, S. Yoon, *J. Power Sources* **2018**, *398*, 193–200; b) X. Zhu, S. Zhou, Q. Yan, S. Wang, *Diamond Relat. Mater.* **2018**, *86*, 87–97.
- [17] Q.-f. Zhao, Y.-h. Yu, Q.-s. Ouyang, M.-y. Hu, C. Wang, J.-h. Ge, S.-q. Zhang, G.-h. Jiang, *Int. J. Electrochem. Sci.* **2022**, *17*, 221142.
- [18] a) Y. Zare, K. Y. Rhee, *JOM* **2023**, *75*, 4485–4493; b) J. A. Torres, Ph.D. thesis, University of California, Los Angeles (United States – California), **2014**, *17*, 3666224.
- [19] a) Y. Yin, L.-J. Wan, W. Du, Y. Guo, *Sci. Sin. Chim.* **2016**, *46*, 1110–1118; b) R. Jiang, C. Cui, H. Ma, *Electrochim. Acta* **2013**, *104*, 198–207.
- [20] M. Z. Wang, M. Tang, S. L. Chen, H. N. Ci, K. X. Wang, L. R. Shi, L. Lin, H. Y. Ren, J. Y. Shan, P. Gao, Z. F. Liu, H. L. Peng, *Adv. Mater.* **2017**, *29*, 1703882.
- [21] L. Gan, M. Dong, Y. Han, Y. Xiao, L. Yang, J. Huang, *ACS Appl. Mater. Interfaces* **2018**, *10*, 18213–18219.
- [22] S. Jin, Y. Jiang, H. Ji, Y. Yu, *Adv. Mater.* **2018**, *30*, 1802014.
- [23] G. Tsoukleri, J. Parthenios, K. Papagelis, R. Jalil, A. C. Ferrari, A. K. Geim, K. S. Novoselov, C. Galloiotis, *Small* **2009**, *5*, 2397–2402.
- [24] Y. Ye, L.-Y. Chou, Y. Liu, H. Wang, H. K. Lee, W. Huang, J. Wan, K. Liu, G. Zhou, Y. Yang, A. Yang, X. Xiao, X. Gao, D. T. Boyle, H. Chen, W. Zhang, S. C. Kim, Y. Cui, *Nat. Energy* **2020**, *5*, 786–793.
- [25] I. Esteve-Adell, M. Porcel-Valenzuela, L. Zubizarreta, M. Gil-Augustí, M. García-Pellicer, A. Quijano-Lopez, *Front. Chem.* **2022**, *10*, 807980.
- [26] a) S. Y. Kim, Y. I. Song, J.-H. Wee, C. H. Kim, B. W. Ahn, J. W. Lee, S. J. Shu, M. Terrones, Y. A. Kim, C.-M. Yang, *Carbon* **2019**, *153*, 495–503; b) J.-Q. Huang, P.-Y. Zhai, H.-J. Peng, W.-C. Zhu, Q. Zhang, *Sci. Bull.* **2017**, *62*, 1267–1274.
- [27] A. Moradpour, M. Kasper, F. Kienberger, *Batteries & Supercaps* **2023**, *6*, e202300155.
- [28] R. Wang, W. Li, L. Liu, Y. Qian, F. Liu, M. Chen, Y. Guo, L. Liu, *J. Electroanal. Chem.* **2019**, *833*, 63–69.
- [29] A. J. Torregrosa, A. Broatch, P. Olmeda, L. Agizza, *Energy* **2023**, *284*, 129316.
- [30] S. Li, S. Tsutsumi, S. Shironita, M. Umeda, *Electrochemistry* **2022**, *90*, 067004–067004.
- [31] T. Shao, C. Li, C. Liu, W. Deng, W. Wang, M. Xue, R. Li, *J. Mater. Chem. A* **2019**, *7*, 1749–1755.

Manuscript received: January 15, 2024

Revised manuscript received: March 27, 2024

Accepted manuscript online: April 2, 2024

Version of record online: May 6, 2024